

Characterizing minimum-length coordinated motions for two discs

David Kirkpatrick and Paul Liu

Abstract

We study the problem of determining optimal coordinated motions for two disc robots in an otherwise obstacle-free plane. Using the total path length traced by the two disc centres as a measure of distance, we give an exact characterization of a shortest collision-avoiding motion for all initial and final configurations of the robots. The individual paths are composed of at most six (straight or circular-arc) segments, and their total length can be expressed as a simple integral with a closed form solution depending only on the initial and final configuration of the robots. Furthermore, the paths can be parametrized in such a way that (i) only one robot is moving at any given time (decoupled motion), or (ii) the angle between the two robots' centres changes monotonically.

1 Introduction

In this paper we consider the problem of planning collision-free motions for two disc robots of arbitrary radius in an otherwise obstacle-free environment. Given two discs \mathbb{A} and \mathbb{B} in the plane, with specified initial and final configurations, we seek a shortest collision-free motion taking \mathbb{A} and \mathbb{B} from their initial to their final configurations. The length of such a motion is defined to be the length sum of paths traced by the centres of \mathbb{A} and \mathbb{B} .

The consideration of disc robots in motion planning has amassed a substantial body of research, the bulk of which is focused on the feasibility, rather than optimality, of motions. Schwartz and Sharir [16] were the first to study motion planning for k discs among polygonal obstacles with n total edges. For $k = 2$, they developed an $\mathcal{O}(n^3)$ algorithm (later improved to $\mathcal{O}(n^2)$ [17, 26]) to determine if a collision-free motion connecting two specified configurations is feasible. When the number of robots k is unbounded, Spirakis and Yap [20] showed that determining feasibility is strongly NP-hard for disc robots, although the proof relies on the robots having different radii. For the analogous problem with rectangular robots, determining feasibility is PSPACE-hard, as shown by Hopcroft et al. [12] and Hopcroft and Wilfong [11]. This result was later generalized by Hearn and Demaine [10] for rectangular robots of size 1×2 and 2×1 .

On the practical side, heuristic and sampling based algorithms have been employed to solve motion planning problem for up to hundreds of robots [15, 21, 25]. These algorithms typically use standard search strategies such as A^* coupled with domain specific heuristics (see [14] and the references contained therein). While efficient in practice, these algorithms are typically numerical or iterative in nature, with no precise performance bounds. A variety of alternative cost measures for our problem has also been considered, such as the minimum time motion under velocity constraints [4, 5, 22] as well as the motion minimizing the total number of continuous movements [1, 3, 6].

A variant of our problem is when the robots are homogeneous and unlabeled. In this case, any robot is allowed to move to any target location, so long as each target position is covered by exactly one robot. For $k = 2$ discs, the unlabeled case is trivial as one can apply our labeled algorithm twice. However, when k is unbounded, Solovey and Halperin [18] show that the unlabeled problem is PSPACE-hard, even in the case of unit squares with polygonal obstacles. Surprisingly, when the robots are located within a simple polygon with no obstacles, a polynomial time for checking feasibility exists [2]. As in the labeled case, a variety of cost measures has been explored for the unlabeled case. Solovey et al. [19] gives an $\tilde{\mathcal{O}}(k^4 + k^2 n^2)$ algorithm that minimizes the length sum of paths traced by the centres of the discs with additive error $4k$. In work by Turpin et al. [22], an optimal solution is found in polynomial time when the cost function is the maximum path length traversed by any single robot. However, their

algorithm requires that the working space is obstacle free and the initial locations of the robots are far enough apart.

This paper makes several novel contributions to the understanding of minimum-length coordinated motions. For the case of two arbitrary discs, we first characterize all initial and final configurations that admit straight-line optimal motions. A special case of this, of course, is where the final configuration is a simple translate of the initial configuration. For all other initial and final configurations, the motion from initial to final configuration involves either a net clockwise or counter-clockwise turn in the relative position of the discs. In this case, our results describe either (i) a single optimal motion, or (ii) two feasible motions, of which one is optimal among all net clockwise motions and the other is optimal among all net counter-clockwise motions. The motions that we describe have bounded curvature except at a constant number of isolated points; in fact, they are composed of a constant number of straight segments and circular arcs, of radius s , the sum of the disc radii. The path length itself can be expressed as a simple integral depending only on the initial and final positions of the discs. Moreover, all paths that we describe can be realized by two different kinds of coordinated motion: *coupled* or *decoupled*. In the coupled motion, the angle formed by a ray joining the two disc centres changes monotonically. Furthermore, the two discs are in contact for a connected interval of time. That is, once the two discs move out of contact, they are never in contact again. In the decoupled motion, only one of the discs moves at any given time.

Our general approach is based on the Cauchy surface area formula, which was first applied to motion planning by Icking et al. [13] to establish the optimality of motions of a directed line segment in the plane, where distance is measured by the length sum of the paths traced by the two endpoints of the segment. This problem has a rich history, and was first posed by Ulam [23] and subsequently solved by Gurevich [9]. Other approaches to that of Icking et al. are quite different, and use control theory to obtain differential equations that characterize the optimal motion [9, 24]. Of course, the problem of moving a directed line segment of length s corresponds exactly to the coordinated motion of two discs with radius sum s constrained to remain in contact throughout the motion. Hence the coordinated motion of two discs with radius sum s can also be seen as the problem of moving an “extensible” line segment that can extend freely but has minimum length s . As such, our results also generalize those of Icking et al. Although we use some of the same tools introduced by Icking et al., our generalization is non-trivial; the doubling argument that lies at the heart of the proof of Icking et al. depends in an essential way on the assumption that the rod length is fixed throughout the motion.

The rest of the paper is organized as follows. In Section 2 we outline some basic definitions as well as our tools for the problem. In Section 3 we summarize the general structure of our proofs, with the main proof and algorithm given in Sections 4 and 5.

2 Background

To describe the motion of a pair of disc robots between their initial and final configurations, we first make precise several terms that have intuitive meaning. We assume for concreteness that the radii of the two discs sum to s .

Definition 2.1. The (instantaneous) **position** of a disc is simply a point in \mathbb{R}^2 specifying the location of its centre. A **placement** of a disc pair (\mathbb{A}, \mathbb{B}) is a pair (A, B) , where A (resp. B) denotes the position of \mathbb{A} (resp. \mathbb{B}). A placement (A, B) is said to be **compatible** if $\|A - B\| \geq s$.

A pair of discs can move from placement to placement through a motion, which we can now define:

Definition 2.2. A **trajectory** $\xi_{\mathbb{A}}$ of a disc \mathbb{A} from a position A_0 to a position A_1 is a continuous, rectifiable curve of the form $\xi_{\mathbb{A}} : [0, 1] \rightarrow \mathbb{R}^2$, where $\xi_{\mathbb{A}}(0) = A_0$, $\xi_{\mathbb{A}}(1) = A_1$.

A **(coordinated) motion** m of a disc pair (\mathbb{A}, \mathbb{B}) from a placement (A_0, B_0) to a placement (A_1, B_1) is a pair $(\xi_{\mathbb{A}}, \xi_{\mathbb{B}})$, where $\xi_{\mathbb{A}}$ (resp. $\xi_{\mathbb{B}}$) is a trajectory of \mathbb{A} (resp. \mathbb{B}) from position A_0 to A_1 (resp. position B_0 to B_1). A motion is said to be compatible or feasible if all of its associated placements are compatible.

Since we are interested in characterizing collision-free motions, we will assume that, unless otherwise specified, all placements and motions that arise in this paper are compatible.

Definition 2.3. The **length** $\ell(\xi_{\mathbb{A}})$ of a trajectory $\xi_{\mathbb{A}}$ is simply the Euclidean arc-length of its trace, that is,

$$\ell(\xi_{\mathbb{A}}) = \sup_T \sum_{i=1}^k \|\xi_{\mathbb{A}}(t_{i-1}) - \xi_{\mathbb{A}}(t_i)\|$$

where the supremum is taken over all subdivisions $T = \{t_0, t_1, \dots, t_k\}$ of $[0, 1]$ where $0 = t_0 < t_1 < \dots < t_k = 1$.

The **length** $\ell(m)$ of a motion m is the sum of the lengths of its associated trajectories, i.e. $\ell(m) = \ell(\xi_{\mathbb{A}}) + \ell(\xi_{\mathbb{B}})$. Finally, the **(collision-free) distance** $d(P_0, P_1)$ between two placements $P_0 = (A_0, B_0)$ and $P_1 = (A_1, B_1)$ is the minimum possible length over all compatible motions m from P_0 to P_1 . We refer to any compatible motion m between P_0 and P_1 satisfying $\ell(m) = d(P_0, P_1)$ as a **shortest** or **optimal** motion between P_0 and P_1 . As a shorthand, we also use $\ell(C)$ to represent the perimeter of a closed curve C .

The fact that d is a metric on the set of placements is easy to check. Nevertheless, one may be concerned about the existence of a shortest motion under this notion of distance. The fact that a shortest motion exists is a consequence of the Hopf-Rinow theorem, for which details can be found in [8].

3 The general approach

Suppose that the disc pair (\mathbb{A}, \mathbb{B}) has initial placement $P_0 = (A_0, B_0)$ and final placement $P_1 = (A_1, B_1)$, and let $m = (\xi_{\mathbb{A}}, \xi_{\mathbb{B}})$ be any motion from P_0 to P_1 . Denote by $\widehat{\xi_{\mathbb{A}}}$ (resp. $\widehat{\xi_{\mathbb{B}}}$) the closed curve defining the boundary of the convex hull of $\xi_{\mathbb{A}}$ (resp. $\xi_{\mathbb{B}}$). Since $\xi_{\mathbb{A}}$ (resp. $\xi_{\mathbb{B}}$), together with the segment $\overline{A_0 A_1}$ (resp. $\overline{B_0 B_1}$), forms a closed curve whose convex hull has boundary $\widehat{\xi_{\mathbb{A}}}$ (resp. $\widehat{\xi_{\mathbb{B}}}$), it follows from convexity that:

$$\ell(\xi_{\mathbb{A}}) \geq \ell(\widehat{\xi_{\mathbb{A}}}) - |\overline{A_0 A_1}| \quad \text{and} \quad \ell(\xi_{\mathbb{B}}) \geq \ell(\widehat{\xi_{\mathbb{B}}}) - |\overline{B_0 B_1}|. \quad (1)$$

When the inequality for $\xi_{\mathbb{A}}$ (resp. $\xi_{\mathbb{B}}$) is an equality, we say that the trace of $\xi_{\mathbb{A}}$ (resp. $\xi_{\mathbb{B}}$) is convex. When both $\xi_{\mathbb{A}}$ and $\xi_{\mathbb{B}}$ are convex, we say that motion $m = (\xi_{\mathbb{A}}, \xi_{\mathbb{B}})$ is convex.

Given a placement $P = (A, B)$, we refer to the angle formed by the vector from B to A with respect to the x -axis as the *angle* of the placement P . Let $[\theta_0, \theta_1]$ be the range of angles counter-clockwise between the angle of P_0 and P_1 .

Observation 3.1. *Let m be any motion from P_0 to P_1 , and let I be the range of angles realized by the set of placements in m . Then $[\theta_0, \theta_1] \subseteq I$ or $S^1 - [\theta_0, \theta_1] \subseteq I$, where $S^1 = [0, 2\pi]$.*

We use Observation 3.1 to categorize the motions we describe into *net clockwise* and *net counter-clockwise* motions. Net clockwise motions satisfy $S^1 - [\theta_0, \theta_1] \subseteq I$ and net counter-clockwise motions satisfy $[\theta_0, \theta_1] \subseteq I$.

Since any motion is either net clockwise or net counter-clockwise (or both) it suffices to optimize over net clockwise and net counter-clockwise motions separately. The following lemma sets out sufficient conditions for net (counter-)clockwise motions to be optimal.

Lemma 3.1. *Let $m = (\xi_{\mathbb{A}}, \xi_{\mathbb{B}})$ be any net (counter-)clockwise motion from P_0 to P_1 satisfying the following properties:*

1. (Convexity) $\widehat{\xi_{\mathbb{A}}} = \xi_{\mathbb{A}} \cup \overline{A_0 A_1}$ and $\widehat{\xi_{\mathbb{B}}} = \xi_{\mathbb{B}} \cup \overline{B_0 B_1}$; and
2. (Minimality) $\ell(\widehat{\xi_{\mathbb{A}}}) + \ell(\widehat{\xi_{\mathbb{B}}})$ is minimized over all possible net (counter-)clockwise motions.

Then m is a shortest net (counter-)clockwise motion from P_0 to P_1 .

Proof. Let $m' = (\xi'_{\mathbb{A}}, \xi'_{\mathbb{B}})$ be any net (counter-)clockwise motion from P_0 to P_1 . It follows from property 1 that $\ell(m) = \ell(\widehat{\xi_{\mathbb{A}}}) - |\overline{A_0 A_1}| + \ell(\widehat{\xi_{\mathbb{B}}}) - |\overline{B_0 B_1}|$. Furthermore, from 2 we know that $\ell(\widehat{\xi_{\mathbb{A}}}) + \ell(\widehat{\xi_{\mathbb{B}}}) \leq \ell(\widehat{\xi'_{\mathbb{A}}}) + \ell(\widehat{\xi'_{\mathbb{B}}})$. Thus, using inequality (1), we have $\ell(m) \leq \ell(\widehat{\xi_{\mathbb{A}}}) - |\overline{A_0 A_1}| + \ell(\widehat{\xi'_{\mathbb{B}}}) - |\overline{B_0 B_1}| \leq \ell(m')$. \square

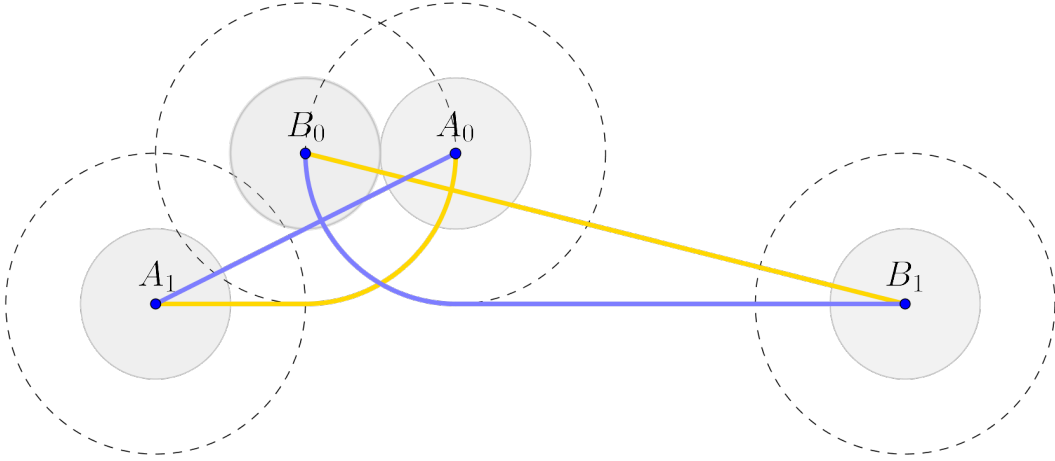


Figure 1: Clockwise (yellow) and counter-clockwise (blue) motions satisfying the two properties of Lemma 3.1.

When a net (counter-)clockwise motion satisfies the two properties of Lemma 3.1, we say it is *(counter-)clockwise optimal*. Figure 1 illustrates two motions from the placement (A_0, B_0) to the placement (A_1, B_1) . The blue motion, where \mathbb{B} first pivots about A_0 and moves to B_1 , followed by \mathbb{A} moving from A_0 to A_1 , is counter-clockwise optimal. The yellow motion, where \mathbb{A} first pivots about B_0 and moves to A_1 , followed by \mathbb{B} moving from B_0 to B_1 , is clockwise optimal (as one can check following the proofs of Sections 4 and 5). However, only the yellow motion is globally optimal.

While property 1 of Lemma 3.1 is typically easy to verify, property 2 is less straightforward and relies indirectly on an application of Cauchy's surface area formula (Theorem 3.2) as well as lower bounds we derive below. Theorem 3.2 allows us to translate the problem of measuring lengths of curves into a problem of measuring the support functions of $\widehat{\xi_{\mathbb{A}}}$ and $\widehat{\xi_{\mathbb{B}}}$ at certain critical angles. Our approach is to lower bound these support functions to get a lower bound on the optimal path length, and then find a motion matching the lower bound.

Definition 3.1. Let C be a closed curve. The *support function* $h_C : S^1 \rightarrow \mathbb{R}$ of C is defined as

$$h_C(\theta) = \sup\{x \cos \theta + y \sin \theta : (x, y) \in C\}.$$

For an angle θ , the set points that realize the supremum above are called *support points*, and the line oriented at angle $\frac{\pi}{2} + \theta$ going through the support points is called the *support line* (see Figure 2).

Theorem 3.2. (Cauchy's surface area formula [7, Section 5.3]) Let C be a closed convex curve in the plane and h_C be the support function of C . Then

$$\ell(C) = \int_0^{2\pi} h_C(\theta) d\theta. \quad (2)$$

As noted in [13], it follows from Theorem 3.2 that we can bound the length of two convex curves in the plane:

Corollary 3.3. Let C_1 and C_2 be closed convex curves in the plane. Then the sum of their lengths can be expressed as follows:

$$\ell(C_1) + \ell(C_2) = \int_0^{2\pi} (h_1(\theta) + h_2(\pi + \theta)) d\theta, \quad (3)$$

where h_i is the support function of C_i .

In order to assert the optimality of our motions, we use the following observations that provide a bound on the support function of an arbitrary motion. Let $h_{\mathbb{A}}$ (resp. $h_{\mathbb{B}}$) denote the support function of $\widehat{\xi_{\mathbb{A}}}$ (resp. $\widehat{\xi_{\mathbb{B}}}$), and let $h_{\mathbb{A}\mathbb{B}}(\theta)$ denote the sum $h_{\mathbb{A}}(\theta) + h_{\mathbb{B}}(\pi + \theta)$. Recall that s is the radii sum of the two discs.

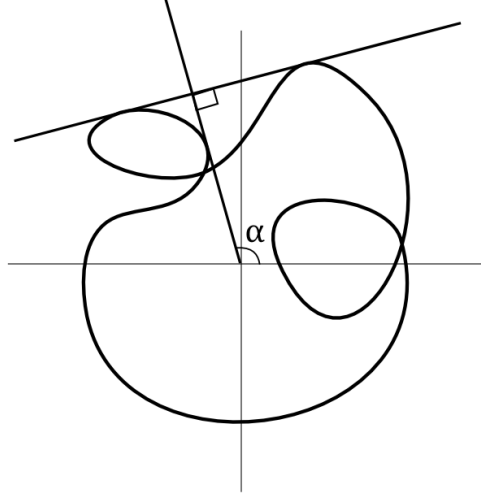


Figure 2: The (two) support points and support line at angle α of a given curve.

Observation 3.2. Let P_0 and P_1 be two configurations and let $[\theta_0, \theta_1]$ be the range of angles counter-clockwise between the angles of P_0 and P_1 . Then, for all net counter-clockwise motions from P_0 to P_1 , and $\theta \in [\theta_0, \theta_1]$, $h_{\mathbb{A}\mathbb{B}}(\theta) \geq s$. Similarly, for all net clockwise motions and $\theta \in S^1 - [\theta_0, \theta_1]$, $h_{\mathbb{A}\mathbb{B}}(\theta) \geq s$.

Observation 3.3. For all support angles, the support function $h_{\mathbb{A}}$ (resp. $h_{\mathbb{B}}$) is lower bounded by the support function $H_{\mathbb{A}}$ (resp. $H_{\mathbb{B}}$) of $\overline{A_0A_1}$ (resp. $\overline{B_0B_1}$), since $\overline{A_0A_1} \subset \widehat{\xi_{\mathbb{A}}}$ (resp. $\overline{B_0B_1} \subset \widehat{\xi_{\mathbb{B}}}$). From this, together with Observation 3.2, it follows that the support function $h_{\mathbb{A}\mathbb{B}}$ is lower bounded point-wise in the counter-clockwise and clockwise cases by

$$\begin{aligned} \max(H_{\mathbb{A}}(\theta) + H_{\mathbb{B}}(\pi + \theta), s \cdot \mathbb{1}_{[\theta_0, \theta_1]}) & \quad (\text{net counter-clockwise}) \\ \max(H_{\mathbb{A}}(\theta) + H_{\mathbb{B}}(\pi + \theta), s \cdot \mathbb{1}_{S^1 - [\theta_0, \theta_1]}) & \quad (\text{net clockwise}) \end{aligned}$$

In the next section we give explicit constructions of optimal motions for many initial-final configuration pairs. This includes, of course, all those whose associated trajectories correspond to two straight segments, what we refer to as **straight-line motions**. In other cases, we construct both the clockwise and counter-clockwise optimal motions, one of which must be optimal among all motions.

4 Optimal paths for two discs

Our constructions of shortest (counter-)clockwise motions can be summarized by the following theorem:

Theorem 4.1. Let \mathbb{A} and \mathbb{B} be two discs with radius sum s in an obstacle-free plane with arbitrary initial and final placements $P_0 = (A_0, B_0)$ and $P_1 = (A_1, B_1)$. Then there is a shortest motion from P_0 to P_1 whose associated trajectories are composed of at most six (straight or circular arcs of radius s) segments.

We devote this entire section to the identification and exhaustive treatment of various cases of Theorem 4.1. The paths that we identify in each case also allow us to provide the following unified characterization of the optimal path length, covering all cases:

Corollary 4.2. Let $H_{\mathbb{A}}$ and $H_{\mathbb{B}}$ be the support functions of the segments $\overline{A_0A_1}$ and $\overline{B_0B_1}$ respectively, $H_{\mathbb{A}\mathbb{B}}(\theta) := H_{\mathbb{A}}(\theta) + H_{\mathbb{B}}(\pi + \theta)$, and m be an optimal motion between P_0 and P_1 . Let $[\theta_0, \theta_1]$ be the range of angles counter-clockwise between P_0 and P_1 . Then

$$\ell(m) = \min \left(\int_0^{2\pi} \max(H_{\mathbb{A}\mathbb{B}}(\theta), s \cdot \mathbb{1}_{[\theta_0, \theta_1]}) d\theta, \int_0^{2\pi} \max(H_{\mathbb{A}\mathbb{B}}(\theta), s \cdot \mathbb{1}_{S^1 - [\theta_0, \theta_1]}) d\theta \right) - |\overline{A_0A_1}| - |\overline{B_0B_1}|$$

where $\mathbb{1}_{[a,b]}$ is the indicator function of the interval $[a, b]$.

Though the expression in Corollary 4.2 looks daunting, the only difference between the two integrals is the indicator function used. The support functions themselves can be expressed in closed form and the integrals are clearly lower bounds on the path length by Corollary 3.3 and Observation 3.3. We emphasize that the integrals can be expressed in closed form if needed, albeit with some cases involved.

We now introduce some additional tools that will help us classify the initial and final placements into different cases.

Definition 4.1. Let p and q be arbitrary points in the plane.

- (a) We denote by $s\text{-circ}(p)$ the circle of radius s centred at point p .
- (b) We denote by $s\text{-corr}(p, q)$ the s -**corridor** associated with p and q , defined to be the Minkowski sum of the line segment \overline{pq} and an open disc of radius s .
- (c) We denote by $s\text{-cone}(p, q)$ the cone formed by all half-lines from p that intersect $s\text{-circ}(q)$.

If disc \mathbb{A} is centred at location A then $s\text{-circ}(A)$ corresponds to the locations forbidden to the centre of disc \mathbb{B} in a compatible placement (see dotted circles in Figure 1). The corridors $s\text{-corr}(A_0, A_1)$ and $s\text{-corr}(B_0, B_1)$ play a critical role in partitioning initial and final placement pairs for which straight-line trajectories (which are clearly optimal) are possible. Specifically, if point $A \notin s\text{-corr}(B_0, B_1)$ then the line segment $\overline{B_0 B_1}$ does not intersect $s\text{-circ}(A)$; i.e. it is possible to translate \mathbb{B} from B_0 to B_1 without interference from disc \mathbb{A} with centre at point A . Similarly, if point $B \notin s\text{-corr}(A_0, A_1)$ it is possible to translate \mathbb{A} from A_0 to A_1 without interference from disc \mathbb{B} with centre at point B .

What follows is a case analysis of various scenarios for the initial and final placements. We first classify the cases by the containment of A_0, A_1, B_0, B_1 within $s\text{-corr}(A_0, A_1)$ and $s\text{-corr}(B_0, B_1)$ (cf. Table 1). While there might appear to be 16 cases — since each point is either contained within a corridor or not — they cluster into just three disjoint collections, referred to as Cases 1, 2 and 3. These are further reduced by symmetries which include (i) interchanging the initial and final placements and (ii) switching the roles of \mathbb{A} and \mathbb{B} .

Case	$A_0 \in s\text{-corr}(B_0, B_1)$	$A_1 \in s\text{-corr}(B_0, B_1)$	$B_0 \in s\text{-corr}(A_0, A_1)$	$B_1 \in s\text{-corr}(A_0, A_1)$	Type of motion
1a	false	*	*	false	straight-line ($B_0 \rightarrow B_1, A_0 \rightarrow A_1$)
1b	*	false	false	*	
2a	true	*	true	*	See Section 5.2
2b	*	true	*	true	
3a	true	true	false	false	See Section 5.3
3b	false	false	true	true	

Table 1: All cases of possible motions. The * entries mean that the specified condition is unconstrained, i.e. it can be either true or false. We leave some cases out due to symmetry.

In all cases our specified motion has a common form – with a possible interchange of the roles of \mathbb{A} and \mathbb{B} . We identify an intermediate position A_{int} (possibly A_0 or A_1) and perform the following sequence of (possibly degenerate) moves:

1. Move \mathbb{A} on the shortest path from A_0 to A_{int} , avoiding $s\text{-circ}(B_0)$;
2. Move \mathbb{B} on the shortest path from B_0 to B_1 , avoiding $s\text{-circ}(A_{\text{int}})$; then
3. Move \mathbb{A} on the shortest path from A_{int} to A_1 , while avoiding $s\text{-circ}(B_1)$.

Without loss of generality, assume that our initial and final configurations have been **normalized** as follows: B_0 and B_1 lie on the x -axis with B_0 at the origin, B_1 right of B_0 . In all but a few special cases, we will only examine

motions that are net counter-clockwise; net clockwise optimal motions can be obtained by reflecting the initial and final placements across the x -axis and then examining net counter-clockwise motions.

The net counter-clockwise orientation of our proposed motion $m = (\xi_{\mathbb{A}}, \xi_{\mathbb{B}})$ as well as the convexity of $\xi_{\mathbb{A}}$ and $\xi_{\mathbb{B}}$ will typically be straightforward to verify. To show the optimality of our motions, we show that the support function of our motions achieves the point-wise lower bound established in Observation 3.3.

4.1 Examples of counter-clockwise optimal motions

Before we attempt to identify optimal motions, it will be instructive to examine a special case, illustrated in Figure 3. This case will provide the simplest non-trivial example of an optimal motion as well as an illustration to the form of our proofs.

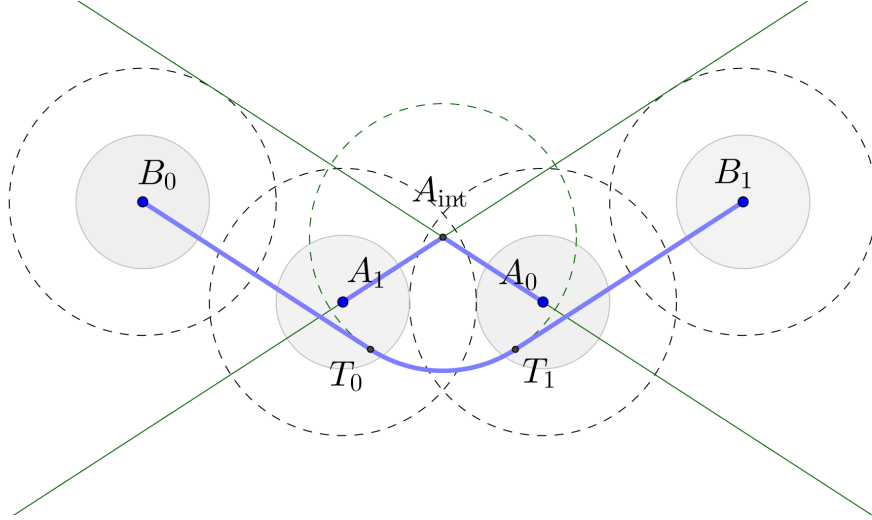


Figure 3

Consider the case shown in Figure 3, where the A_i 's are in $s\text{-corr}(B_0, B_1)$, the B_i 's are on the x -axis, and the A_i 's are symmetric about the perpendicular bisector of $\overline{B_0B_1}$.

We define some points useful to our construction of the optimal motion. Let a_0 and a_1 be the upper tangents from A_0 to $s\text{-circ}(B_0)$, and A_1 to $s\text{-circ}(B_1)$ respectively. These two tangents intersect in a point A_{int} on the perpendicular bisector of $\overline{B_0B_1}$. Let b_0 and b_1 be the lower tangents from B_0 and B_1 to $s\text{-circ}(A_{\text{int}})$ respectively, and let T_0 and T_1 be intersection points of b_0 and b_1 with $s\text{-circ}(A_{\text{int}})$. Note that by construction, a_0 is parallel to b_1 and a_1 is parallel to b_0 .

Claim 4.3. *The following is a counter-clockwise optimal motion (see bolded outline in Figure 3):*

1. Move \mathbb{A} from A_0 to A_{int} ;
2. Move \mathbb{B} from B_0 to B_1 , avoiding $s\text{-circ}(A_{\text{int}})$. This involves translating \mathbb{B} from B_0 to T_0 , rotating around $s\text{-circ}(A_{\text{int}})$ in a range of angles $[\beta_0, \beta_1]$, and finally translating from T_1 to B_1 ; then
3. Move \mathbb{A} from A_{int} to A_1 .

Proof. It is easy to check that property 1 (convexity) of Lemma 3.1 is satisfied. To show that property 2 (minimality) holds as well we verify that $h_{\mathbb{A}\mathbb{B}}(\theta)$ matches its lower bound. By Observation 3.3, we may check that for all angles θ , either $h_{\mathbb{A}\mathbb{B}}(\theta) = s$ for θ in the range of angles counter-clockwise between the initial and final placement, or is determined by \mathbb{A} and \mathbb{B} in their initial or final position.

By construction, β_0 is normal to the orientation of b_0 (as well as a_0) and β_1 is normal to b_1 (as well as a_1). This ensures that for the range of angles $[\beta_0, \beta_1]$, A_{int} is the support point of $h_{\mathbb{A}}(\theta)$ while the support point of $h_{\mathbb{B}}(\theta + \pi)$ lies on the arc of the circle traversed by \mathbb{B} . Hence $h_{\mathbb{A}\mathbb{B}}(\theta) = s$ for $\theta \in [\beta_0, \beta_1]$.

Furthermore, A_{int} is only a support point for angles in $[\beta_0, \beta_1]$, since \mathbb{A} moves along tangents a_0 and a_1 . Thus for angles in $S^1 - [\beta_0, \beta_1]$, either A_0 or A_1 must be one support point, and either B_0 or B_1 must be the other. \square

Remark 4.1.1. *Even if the positions of A_0 and A_1 were swapped in the motion above, the trace of the optimal counter-clockwise motion would remain the same. The proof of optimality would proceed as above, using instead the tangents from A_0 to B_1 and A_1 to B_0 as a_1 and a_0 respectively.*

In the proof above, A_{int} remains a support during the angles of \mathbb{B} 's rotation even if we shift it slightly vertically upwards.¹ This motivates the following definition:

Definition 4.2. Let p be a point in $s\text{-corr}(B_0, B_1)$. Let \mathcal{R} be the region below both upper tangents from p to B_0 and B_1 . We call \mathcal{R} the **dominated region** of p with respect to $s\text{-corr}(B_0, B_1)$. For any point $q \in \mathcal{R}$, we say that p **dominates** q .

Note that if p dominates A_0 and A_1 , then substituting p for A_{int} in the proposed motion for Figure 3 would maintain the property that the support function $h_{\mathbb{A}\mathbb{B}}(\theta)$ is exactly s in the angles of \mathbb{B} 's rotation. In fact, we have the following general lemma:

Lemma 4.4. *Let p be any point that dominates A_0 and A_1 , and let m be any motion of the form:*

1. *Move \mathbb{A} from A_0 to p in a motion m_1 , staying entirely within the region dominated by p ;*
2. *Move \mathbb{B} on the shortest path from B_0 to B_1 that travels below $s\text{-circ}(p)$. This involves moving \mathbb{B} on a tangent segment b_0 from B_0 to $s\text{-circ}(p)$, rotating around $s\text{-circ}(A_{\text{int}})$ in a range of angles $[\beta_0, \beta_1]$, and moving on a tangent segment b_1 from $s\text{-circ}(p)$ to B_1 ; then*
3. *Move \mathbb{A} from p to A_1 in a motion m_2 , staying entirely within the region dominated by p .*

For any such motion m , $h_{\mathbb{A}\mathbb{B}}(\theta) = s$ for $\theta \in [\beta_0, \beta_1]$. Furthermore, if m_1 and m_2 form a convex trace when concatenated together, and the tangents of m_1 and m_2 at p are parallel to b_1 and b_0 respectively, then p is a support point iff the support angle is in the range $[\beta_0, \beta_1]$.

Proof. The proof follows exactly the same analysis as the argument for A_{int} in the proof of Claim 4.3, substituting the tangents of m_1 and m_2 at p for a_0 and a_1 . \square

Lemma 4.4 will allow us to exploit the commonality in many of the proofs we use in subsequent cases, as most motions will involve rotating around at least 1 pivot.

As an example, consider Figure 4, which shows an optimal counter-clockwise motion that we'll encounter in Case 2. In this motion, \mathbb{A} first moves from A_0 to A_{int} , followed by \mathbb{B} rotating from B_0 to B_1 , and finished by moving A_{int} to A_1 . Lemma 4.4 allows us to immediately say that A_{int} is a support point exactly when \mathbb{B} rotates from B_0 to B_1 , since the motions from A_0 and A_1 to A_{int} stay within the region dominated by A_{int} . The motion is also optimal, as the combined movement of \mathbb{A} is convex, and the tangents at A_{int} are parallel to the tangents of $s\text{-circ}(A_{\text{int}})$ at B_0 and B_1 .

4.2 Certifying non-optimality of counter-clockwise motions

The proofs we use in our case analysis will largely resemble the special case discussed in Section 4.1. Nevertheless for certain configurations, the tools we've developed in the previous section seem unable to show the optimality of net counter-clockwise motions. In such situations, we will show that the optimal net clockwise motion is shorter than any net counter-clockwise motion. In this section we analyse another special case, which will lead us to a set of placements for which we can prove that the optimal motion is net clockwise. This will help us deal with

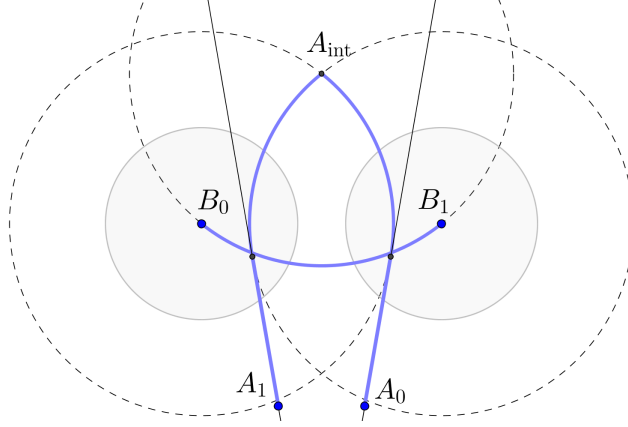


Figure 4

subcases for which the demonstration of net counter-clockwise optimal motions seems to be beyond the reach of our techniques.

Let us consider a variant of Figure 3 where the B_i 's are now closer together, as depicted in Figure 5 and the positions of A_0 and A_1 are swapped. Again, we may draw the appropriate upper-tangents from the A_i 's and compute an intermediate point A_{int} . By Lemma 4.4, the trace length of the “motion” m' outlined in Figure 5 is no greater than that of any net-counter-clockwise motion. However, the trace given in Figure 5 is not feasible, as it requires A_0 to move through $s\text{-circ}(B_0)$. In this case, we do not know of any counter-clockwise optimal motion for which optimality can be shown with Cauchy's surface area formula. As it turns out, we may sidestep this apparent difficulty by considering clockwise optimal motions.

Claim 4.5. *The optimal motion to Figure 5 is net clockwise.*

Proof. Consider the trace shown in Figure 6, where A'_{int} is the point A_{int} reflected vertically across the segment $\overline{B_0 B_1}$. The following motion m is a feasible realization of this trace:

1. Move \mathbb{A} from A_0 to the point A' vertically below A'_{int} , on the along the segment $\overline{A_0 A_1}$;
2. Move \mathbb{B} from B_0 to B_1 , rotating across the top of $s\text{-circ}(A'_{\text{int}})$; then
3. Move \mathbb{A} to A_1 .

It is easy to see that $\ell(m) < \ell(m')$: the total distance traveled by \mathbb{B} is the same in m and m' , whereas the total distance traveled by \mathbb{A} is strictly less in m . Since m' was a lower bound for all counter-clockwise optimal motions, this implies that any clockwise optimal motion would be shorter than a counter-clockwise one. Thus we may restrict our attention to clockwise optimal motions only. \square

The intermediate point, A' was not strictly necessary here as we could have also moved A_0 straight to A_1 on the first step. In constructing the lower bounds below however, we will make use of a judiciously chosen intermediate point.

In any case we shall encounter, the clockwise optimal motion is similar to counter-clockwise motions we've already considered. For this case, the optimal clockwise motion looks like a vertically reflected version of Figure 3. The intermediate pivot point A_{int} is formed by using the intersection of lower tangents from the A_i 's to the $s\text{-circ}(B_j)$'s, where $i \neq j$. In general, we have the following lemma:

¹However, the shifted A_{int} is a support outside of the angles of rotation as well, which means $h_{\mathbb{A}\mathbb{B}}$ does not achieve its lower bound outside of $[\beta_0, \beta_1]$.

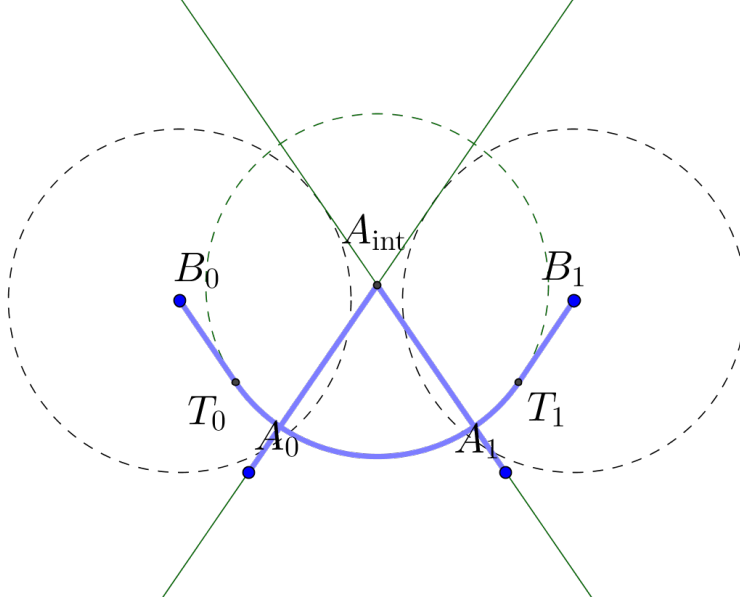


Figure 5

Lemma 4.6. *Suppose $A_0, A_1 \in s\text{-corr}(B_0, B_1)$ and let H_{ij} denote the half space below the upper tangent from A_i to $s\text{-circ}(B_j)$. If H_{ij} intersects $s\text{-circ}(B_i)$ for some $i \in \{0, 1\}$, $j = 1 - i$, and $A_j \in H_{ij}$, then the optimal motion must be net clockwise.*

Proof. There are two major cases: (i) the case where $s\text{-circ}(B_0)$ does not intersect $s\text{-circ}(B_1)$ and (ii) the case where they do intersect. For both cases, we assume that A_0 is under the line connecting B_0 with B_1 . The other cases are treated similarly with almost exactly the same proof.

$s\text{-circ}(B_0)$ does not intersect $s\text{-circ}(B_1)$ Let U_0 be the upper tangent point of A_0 to $s\text{-circ}(B_1)$. By our assumptions, A_1 lies below $\overline{A_0U_0}$, and $A_1 \in s\text{-corr}(B_0, B_1)$. Let U_1 be the upper tangent point of A_1 to $s\text{-circ}(B_0)$. We first deal with the case where the tangent segments $\overline{A_0U_0}$ and $\overline{A_1U_1}$ intersect at a point $A_{\text{int}} \in s\text{-corr}(B_0, B_1)$ (see Figure 7).

Consider the following “motion” $m' = (\xi'_A, \xi'_B)$:

1. Move A on a straight line from A_0 to A_{int} .
2. Move B from B_0 to B_1 avoiding $s\text{-circ}(A_{\text{int}})$. This involves moving B to T_0 (the lower tangent point of B_0 and $s\text{-circ}(A_{\text{int}})$), rotating B counter-clockwise about A_{int} to T_1 (the lower tangent point of B_1 and $s\text{-circ}(A_{\text{int}})$) in a range of angles $[\beta_0, \beta_1]$, and then moving B from T_1 to B_1 .
3. Move A in a straight line from A_{int} to A_1 .

The “motion” outlined above is infeasible, as the position of B_0 prevents the movement from A_0 to A_{int} in a straight-line. However, Lemma 4.4 shows that $\ell(m')$ forms a lower bound on all possible net clockwise motions.

Now we construct a net clockwise motion whose length is no greater than that of m' . Construct the point A'_{int} in Figure 7, which is the result of two reflections of A_{int} , first along the line from B_0 to B_1 and then along the perpendicular bisector of $\overline{B_0B_1}$. Consider the following motion m :

1. Move B from B_0 to B_1 avoiding $s\text{-circ}(A'_{\text{int}})$ by rotating over the top of it.
2. Move A_0 to A_1 in a straight line.

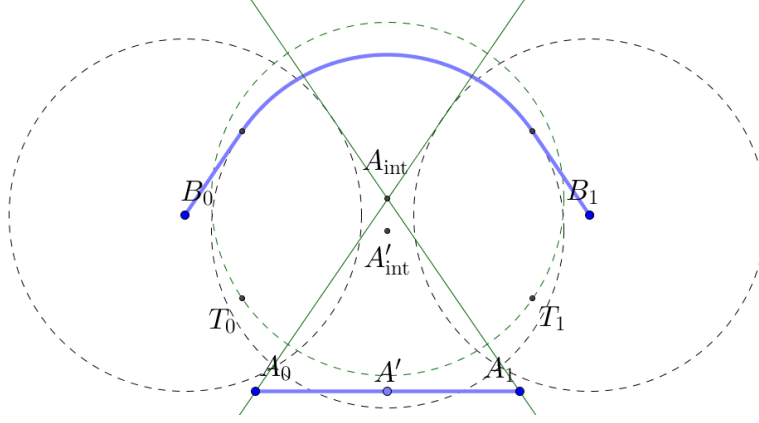


Figure 6

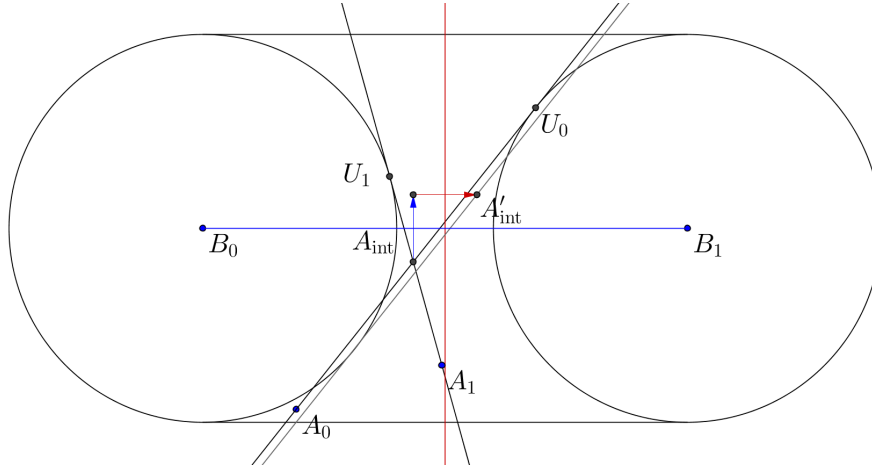


Figure 7: A case of Lemma 4.6.

Clearly step 1 of m is the same length as step 2 of m' , and step 2 of m is at most the length of steps 1 and 3 of m' , so $\ell(m) \leq \ell(m')$. Furthermore m is a feasible motion. To see this, let t be line through A'_{int} parallel to the segment $\overline{A_0 A_{\text{int}}}$, and let q be the tangent point between $s\text{-circ}(B_0)$ and t . Note that A'_{int} lies on the right of q above t and A_0 is left of q and above t , so A_0 does not obstruct the movement of \mathbb{B} in step 1.

Hence the optimal motion must be net clockwise in the case where $\overline{A_0 U_0}$ and $\overline{A_1 U_1}$ intersect.

When $\overline{A_0 U_0}$ and $\overline{A_1 U_1}$ do not intersect (see Figure 8), this means that U_1 is below $\overline{A_0 U_0}$. In this case, let A_{int} be the right-most intersection point between $\overline{A_0 U_0}$ and $s\text{-circ}(B_0)$ and the proof above will work without modification.

$s\text{-circ}(B_0)$ intersects $s\text{-circ}(B_1)$ We now deal with case (ii), where $s\text{-circ}(B_0)$ intersects $s\text{-circ}(B_1)$ (see Figure 9). Let \mathcal{L} (resp. \mathcal{U}) denote the region within $s\text{-corr}(B_0, B_1)$ below (resp. above) the discs enclosed by $s\text{-circ}(B_0)$ and $s\text{-circ}(B_1)$. We will show that if both A_0 and A_1 are in \mathcal{L} , then the optimal motion must be net clockwise. The case for \mathcal{U} can be handled similarly.

As before, we will first lower bound the optimal net counter-clockwise motion by an infeasible motion, and then show a net clockwise motion that is at most the length of the lower bound.

Let t be the upper intersection point of $s\text{-circ}(B_0)$ and $s\text{-circ}(B_1)$. If A_0 is left of the perpendicular bisector of $\overline{B_0 B_1}$, then define the following: U_0 is the upper tangent point of A_0 to $s\text{-circ}(B_1)$, U_1 is the upper tangent point of A_1 to $s\text{-circ}(B_0)$. If A_1 is right of the perpendicular bisector, let U_0 be the upper tangent point of A_0 to $s\text{-circ}(B_0)$,

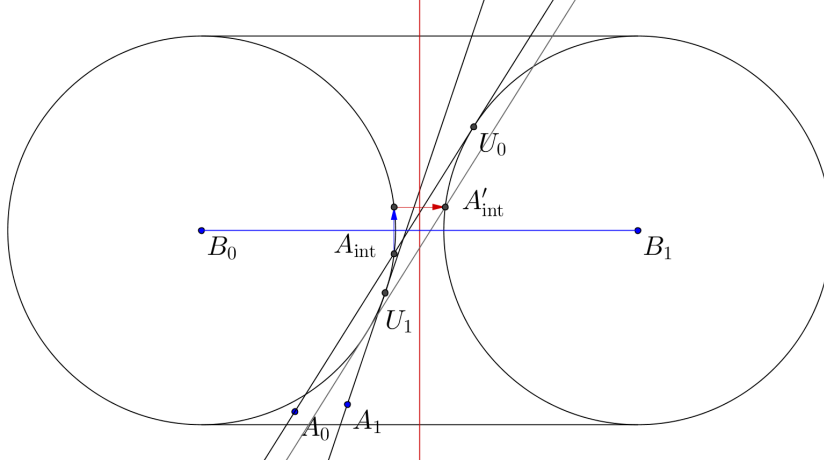


Figure 8: A case of Lemma 4.6.

and let U_1 be the upper tangent point of A_1 to $s\text{-circ}(B_1)$.

If U_1 is counter-clockwise of t on $s\text{-circ}(B_0)$ or U_0 is clockwise of t on $s\text{-circ}(B_1)$, one can check that the proof of the non-intersecting case works here as well. Otherwise, both U_0 and V_1 are vertically below t .

In this case, consider the following “motion” m' :

1. Move \mathbb{A} on a straight line from A_0 to t . This involves possibly moving on a chord through $s\text{-circ}(B_0)$ and $s\text{-circ}(B_1)$ in a range of angles $[\alpha_0, \alpha_1]$.
2. Move \mathbb{B} from B_0 to B_1 avoiding $s\text{-circ}(t)$.
3. Move \mathbb{A} in a straight line from t to A_1 . This involves possibly moving on a chord through $s\text{-circ}(B_0)$ and $s\text{-circ}(B_1)$ in a range of angles $[\alpha_2, \alpha_3]$.

As in the previous case, Lemma 4.4 (with t as the dominating point) shows that $\ell(m')$ forms a lower bound on all net counter-clockwise motions.

Now we construct a net clockwise motion whose length is no greater than that of m' . Construct the point A'_{int} , which is the vertical reflection of t across $\overline{B_0B_1}$. Now consider the same type of motion m that we used in the non-intersecting case:

1. Move \mathbb{B} from B_0 to B_1 avoiding $s\text{-circ}(A'_{\text{int}})$ by rotating over the top of it.
2. Move A_0 to A_1 in a straight line.

Clearly m is a feasible motion. As before, step 1 of m is the same length as step 2 of m' , and step 2 of m is at most the length of steps 1 and 3 of m' , so $\ell(m) \leq \ell(m')$. \square

5 Case analysis of counter-clockwise optimal motions

In this section we treat exhaustively each case of Table 1, beginning with Case 1. For Case 2 and onwards, the general form of the motion we construct will be similar to examples presented in Section 4. That is, the motion will be decoupled, consisting of at most two \mathbb{A} motions which meet at an intermediate point A_{int} and one \mathbb{B} motion. The motions themselves are constructed from tangent segments and arcs of radius s circles. When an arc of a circle is part of a motion, the centre of the circle will be dominating in the sense of Definition 4.2.

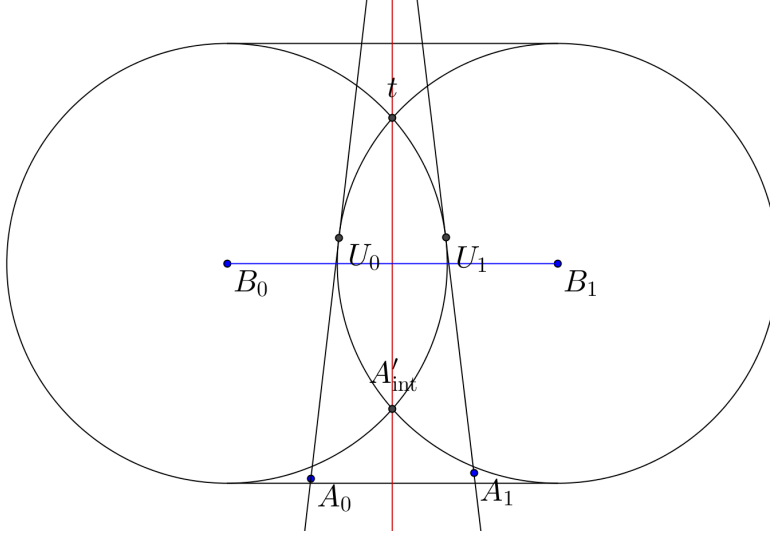


Figure 9: A case of Lemma 4.6.

5.1 Case 1

It suffices to treat Case 1a, as Case 1b reduces to Case 1a by symmetry. In Case 1a, $A_0 \notin s\text{-corr}(B_0, B_1)$, so on the first step we translate \mathbb{B} from B_0 to B_1 in a straight line without touching \mathbb{A} . At this point \mathbb{A} can move freely in a straight line from A_0 to A_1 , as $B_1 \notin s\text{-corr}(A_0, A_1)$. As we shall see through examining the other cases, Case 1 is the only situation where a straight-line motion is possible.

5.2 Case 2

It suffices to treat Case 2a since Case 2b reduces to 2a by symmetry; thus we assume that $A_0 \in s\text{-corr}(B_0, B_1)$ and $B_0 \in s\text{-corr}(A_0, A_1)$. In fact, we can relax this and assume that $A_1 \in s\text{-cone}(A_0, B_0)$. This amounts to including the “wedge” between A_0 and $s\text{-circ}(B_0)$.

The motion we take in Case 2a depends on the zone in which A_1 lies (cf. Figure 10 and 14). Each zone represents a locus of locations for A_0 which give rise to a specific sequence of motions that are counter-clockwise optimal within that zone.

Let p be the upper tangent point from A_0 to $s\text{-circ}(B_0)$. The zones are defined by the following properties:

- Zone I: The set of points $q \in s\text{-cone}(A_0, B_0)$ for which some tangent point from q to $s\text{-circ}(B_0)$ lies on the arc of $s\text{-circ}(B_0)$ from p to u .
- Zone II: The set of points $q \in s\text{-cone}(A_0, B_0)$ where the tangent from q to $s\text{-circ}(B_1)$ intersects the arc of $s\text{-circ}(B_0)$ from p to u .
- Zone III: The set of points $q \in s\text{-cone}(A_0, B_0)$ where the tangent from q to $s\text{-circ}(B_1)$ intersects $\overline{A_0 p}$.
- Zone IV: The set of points $q \in s\text{-cone}(A_0, B_0)$ that are dominated by t . t is A_0 if $A_0 \notin s\text{-circ}(B_1)$, is the intersection point of $\overline{A_0 p}$ and $s\text{-circ}(B_1)$ if $A_0 \in s\text{-circ}(B_1)$, and is the upper intersection point of $s\text{-circ}(B_0)$ and $s\text{-circ}(B_1)$ if the intersection point of the circles lie on the arc from p to u .

For concreteness, we also give constructive definitions in each subcase below.

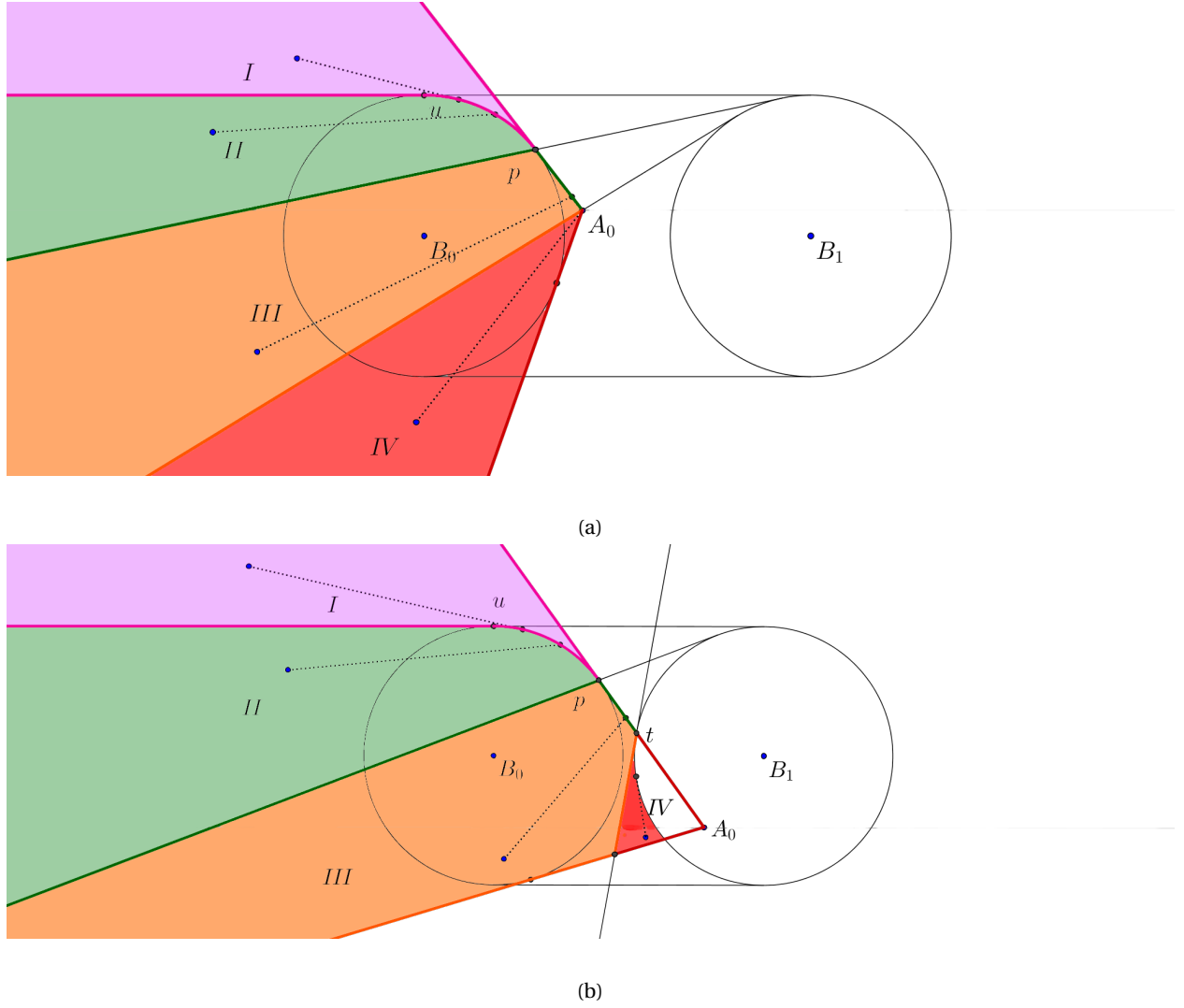


Figure 10: The different zones of Case 2 when $s\text{-circ}(B_0)$ and $s\text{-circ}(B_1)$ do not intersect. We have different optimal motions (dotted lines) depending on the zone in which A_1 lies.

5.2.1 Subcase 1: $s\text{-circ}(B_0)$ and $s\text{-circ}(B_1)$ do not intersect

We first discuss the constructions of zones I-IV in Figures 10a and 10b. We may construct zones I-IV explicitly through the following tangents and curves:

1. The horizontal tangent through the uppermost point u of $s\text{-circ}(B_0)$. This tangent and the arc of $s\text{-circ}(B_0)$ between u and p (where p is the upper tangent point between A_0 and $s\text{-circ}(B_0)$) separates zone I from zone II.
2. The tangent through p to $s\text{-circ}(B_1)$. This tangent separates zone II from zone III.
3. If $A_0 \notin s\text{-circ}(B_1)$, the tangent line from A_0 to $s\text{-circ}(B_1)$ (cf. Figure 10a). Otherwise, the tangent of $s\text{-circ}(B_1)$ through t , where t is the intersection point of $\overline{A_0 p}$ and $s\text{-circ}(B_1)$ (cf. Figure 10b). This tangent separates zone III from zone IV.

Note that zone III and IV may be empty, if the position of A_0 lies below the line tangent to the bottom of $\text{circ}_s(B_0)$ and the top of $\text{circ}_s(B_1)$.

For each zone we specify the location of the intermediate point A_{int} as follows:

Zone I: A_{int} is the point A_1 .

Zone II: A_{int} is the rightmost point of intersection between the tangent from A_1 to $\text{circ}_s(B_1)$ and $\text{circ}_s(B_0)$.

Zone III: A_{int} the point of intersection of the tangent from A_1 to $\text{circ}_s(B_1)$ and the tangent from A_0 to $\text{circ}_s(B_0)$.

Zone IV: A_{int} is the point t (as defined above).

We define points T_0 and T_1 which are the lower points of tangency to $\text{circ}_s(A_{\text{int}})$ from B_0 and B_1 respectively. Our three-step generic motion involves:

1. Moving \mathbb{A} on the shortest path from A_0 to A_{int} , avoiding $\text{circ}_s(B_0)$. This may involve rotating \mathbb{A} counter-clockwise about B_0 in a range of angles $[\alpha_0, \alpha_1]$.
2. Moving \mathbb{B} from B_0 to B_1 avoiding $\text{circ}_s(A_{\text{int}})$. This involves translating \mathbb{B} from B_0 to T_0 , rotating \mathbb{B} counter-clockwise about A_{int} from T_0 to T_1 in a range of angles $[\beta_0, \beta_1]$, and then translating \mathbb{B} from T_1 to B_1 .
3. Translating \mathbb{A} from A_{int} to A_1 (collision-free by the disjointness of $\text{cone}_s(A_0, B_0)$ and $\text{circ}_s(B_1)$).

From the descriptions above, one can see that there is some amount of symmetry between zone I and IV. For this reason, we first dispense with Zones II and III, and then handle Zone I and IV at the end of this section.

A_1 is in zone II

If A_1 is in zone II, then the tangent from A_1 to B_1 must intersect B_0 in up to two points. Let A_{int} be the rightmost intersection point.

Proof. Since B_0 dominates B_1 with respect to $s\text{-corr}(A_0, A_1)$, we have by Lemma 4.4 that $h_{\mathbb{A}\mathbb{B}}(\theta) = s$ for $\theta \in [\alpha_0, \alpha_1]$. Similarly, since A_{int} dominates A_0 and A_1 with respect to $s\text{-corr}(B_0, B_1)$, $h_{\mathbb{A}\mathbb{B}}(\alpha) = s$ for $\alpha \in [\beta_0, \beta_1]$ by Lemma 4.4.

For angles in $S^1 - [\alpha_0, \alpha_1] - [\beta_0, \beta_1]$, one can check that A_0 or A_1 must be one support point, and either B_0 or B_1 must be the other. \square

A_1 is in zone III

Proof. By construction, A_{int} dominates A_0 and A_1 with respect to $s\text{-corr}(B_0, B_1)$. Hence by Lemma 4.4, we have $h_{\mathbb{A}\mathbb{B}}(\theta) = s$ for $\theta \in [\alpha_0, \alpha_1]$. For angles in $S^1 - [\alpha_0, \alpha_1]$, one can see that either A_0 or A_1 must be one support point, and either B_0 or B_1 must be the other. \square

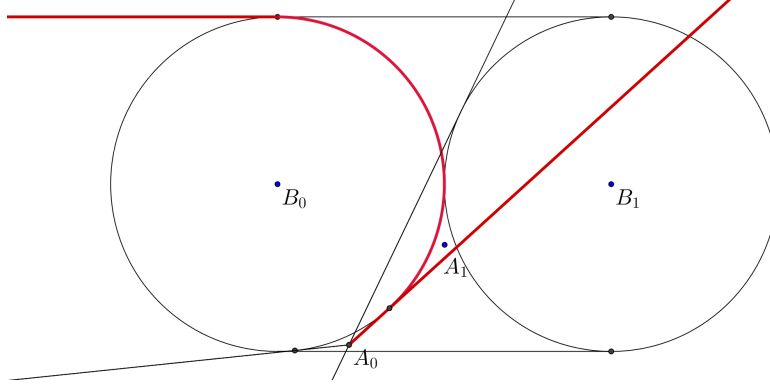


Figure 11: Zone I, example of when A_1 is below U . Zone I is outlined by the bolded tangents.

A_1 is in zone I

There are two cases for Zone I, the location of A_1 with respect to the upper tangent A_0 and $s\text{-circ}(B_1)$. Let U be the upper tangent of A_0 and $s\text{-circ}(B_1)$.

A_1 is above U .

Proof. In this case, A_1 either dominates A_0 or is outside of $s\text{-corr}(B_0, B_1)$ and so by Lemma 4.4 choosing A_1 as A_{int} shows that $h_{\mathbb{A}\mathbb{B}}(\theta) = s$ for $\theta \in [\beta_0, \beta_1]$ (where $[\beta_0, \beta_1] = \emptyset$ for $A_1 \notin s\text{-corr}(B_0, B_1)$). Furthermore, B_0 dominates B_1 with respect to $s\text{-corr}(A_0, A_1)$, so Lemma 4.4 again shows that $h_{\mathbb{A}\mathbb{B}}(\theta) = s$ for $\theta \in [\beta_0, \beta_1]$. Since there are no intermediate pivot points except for the A_i 's and B_i 's, it's clear that for all other angles, A_0 or A_1 must be one support and B_0 or B_1 must be the other. \square

A_1 is below U . In this case (see Figure 11), the positions of A_0 and A_1 satisfy the conditions of Lemma 4.6. Thus we may look for a clockwise motion. In the clockwise zones, A_1 is in Zone IV of A_0 , which we handle below.

A_1 is in zone IV

Due to the complexity of Zone IV, we split it into three subcases.

Zone IV, subcase 1. We first handle the cases for which $A_0 \notin s\text{-circ}(B_1)$ and the upper tangent point of A_1 and $s\text{-circ}(B_1)$ lies inside $s\text{-corr}(B_0, B_1)$. By these assumptions, we must have $A_1 \in s\text{-corr}(B_0, B_1)$ or below the lower horizontal tangent of $s\text{-circ}(B_0)$ and $s\text{-circ}(B_1)$ (see Figure 12).

In this case, choosing A_{int} to be A_0 in our three-step generic motion yields a net optimal counter-clockwise motion.

Proof. By construction of Zone IV, A_0 dominates A_1 with respect to $s\text{-corr}(B_0, B_1)$. Hence by Lemma 4.4, $h_{\mathbb{A}\mathbb{B}}(\alpha) = s$ for $\alpha \in [\alpha_0, \alpha_1]$.

By our property that the upper tangent point of A_1 and $s\text{-circ}(B_1)$ lies inside $s\text{-corr}(B_0, B_1)$, we have that B_1 dominates B_0 with respect to $s\text{-corr}(A_0, A_1)$.

For angles in $S^1 - [\alpha_0, \alpha_1] - [\beta_0, \beta_1]$, either A_0 or A_1 must be one support point, and either B_0 or B_1 must be the other. This is due to the fact that all pivot points in our motion are either the initial or final positions, and all non-pivots were either circular arcs or tangents. \square

This is exactly the motion in Zone IV, subcase 1, with the roles of A and B switched, so the optimality of this motion is already shown above.

Zone IV, subcase 3. If subcase 1 and subcase 2 do not apply, then $A_0 \in s\text{-circ}(B_1)$ (cf. Figure 10b).

In this case the optimal option is:

1. Move \mathbb{A} on a straight line from A_0 to t .
2. Move \mathbb{B} from B_0 to B_1 avoiding $s\text{-circ}(t)$. This involves moving \mathbb{B} to T_0 , rotating \mathbb{B} counter-clockwise about A_{int} to T_1 in a range of angles $[\alpha_0, \alpha_1]$, and then moving \mathbb{B} from T_1 to B_1 .
3. Move \mathbb{A} on a shortest path from t to A_1 while avoiding $s\text{-circ}(B_1)$. This involves rotating possibly rotating \mathbb{A} in a range of angles $[\beta_0, \beta_1]$ around $s\text{-circ}(B_1)$.

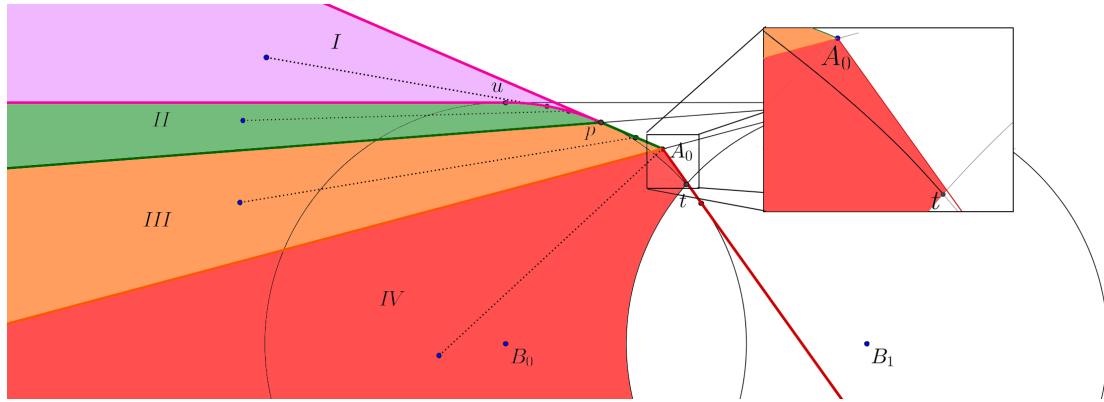
In this case, the motion is of the same type as the one given for Zone II and the exact same proof applies.

5.2.2 Subcase 2: $s\text{-circ}(B_0)$ and $s\text{-circ}(B_1)$ intersect

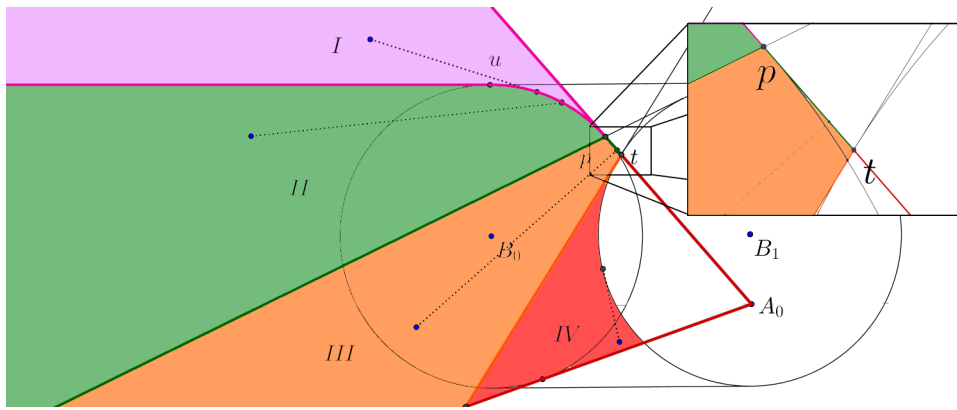
When $s\text{-circ}(B_0)$ and $s\text{-circ}(B_1)$ intersect (cf. Figure 14), the zones are defined by the following curves:

1. The two tangents from A_0 to $s\text{-circ}(B_0)$.
2. The horizontal tangent from the top of $s\text{-circ}(B_0)$.
3. The tangent from p to $s\text{-circ}(B_1)$ where p is the upper tangent point from A_0 to $s\text{-circ}(B_0)$.
4. The tangent line from t to $s\text{-circ}(B_1)$. Let v be the intersection point of the line from A_0 to p and $s\text{-circ}(B_1)$. If $A_0 \notin s\text{-circ}(B_1)$, then t is A_0 . Otherwise, $A_0 \in s\text{-circ}(B_1)$ and t is v when p lies outside of the $s\text{-circ}(B_1)$ (Figure 14b), and t is the upper intersection point between the $s\text{-circ}(B_i)$'s otherwise (Figure 14c).

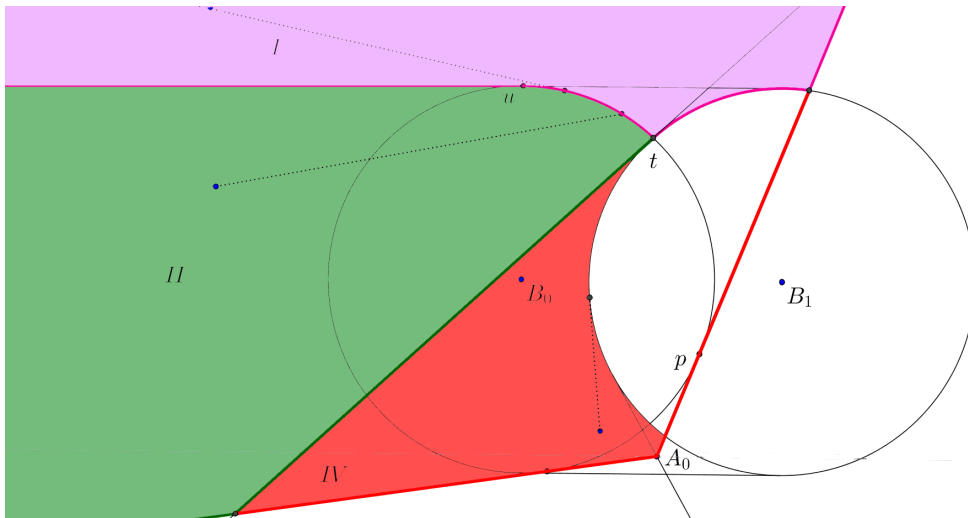
For the most part, the motions executed in Subcase 1 and Subcase 2 are the same, as are their intermediate points. However, for Zone I and IV there are small differences, as we shall see.



(a)



(b)



(c)

Figure 14: The different zones of Case 2 when $s\text{-circ}(B_0)$ and $s\text{-circ}(B_1)$ intersect. We have different optimal motions (dotted lines) depending on the zone in which A_1 lies.

A_1 is in zone II or III

In these zones, the motion is the same as the non-intersecting case.

A_1 is in zone I

By Lemma 4.6, if A_1 is located in any portion of Zone I which intersects the region below the $s\text{-circ}(B_i)$'s, then the motion must be net-clockwise optimal (an example can be found in Figure 11, with the B_i 's pushed closer together). In this case, A_1 is in Zone IV of the clockwise zones, which we handle below. Otherwise, the motion for Zone I is the same as in Subcase 1, and the same proof applies.

A_1 is in zone IV

Here we divide the motion into two different cases, depending on whether we are in Figure 14a, or 14b and Figure 14c. To be precise, denote \mathcal{U} to be the region of $s\text{-corr}(B_0, B_1)$ that is above the $s\text{-circ}(B_i)$'s. We divide into two cases, depending on whether $A_0 \in \mathcal{U}$ or not.

Zone IV, subcase 1. $A_0 \in \mathcal{U}$ In this case, the motions are exactly the same as those for Zone IV of the non-intersecting case.

Zone IV, subcase 2. $A_0 \notin \mathcal{U}$ This case is shown in Figures 14b and 14c. First, if A_1 is right of the upper tangent between A_0 and $s\text{-circ}(B_1)$ and left of the upper tangent between A_0 and $s\text{-circ}(B_0)$, then Lemma 4.6 shows that the optimal motion must be clockwise. In this case, the optimal clockwise motion is:

1. Move \mathbb{B} from B_0 to B_1 rotating over the top of $s\text{-circ}(A_0)$.
2. Move \mathbb{A} in a straight line from A_0 to A_1 .

Proof. The optimality of this motion can be seen by reflecting the configuration vertically. Since A_0 dominates A_1 , Lemma 4.4 shows that $h_{\mathbb{A}\mathbb{B}}(\theta) = s$ in the angles of rotation. For all other angles, the two support points are either A_0 or A_1 and B_0 or B_1 . \square

Now we assume that A_1 is outside of the region handled above. Let T_0 and T_1 be the lower tangent points of B_0 and B_1 to $s\text{-circ}(t)$ respectively. Let V_0 be the upper tangent point between t and $s\text{-circ}(B_0)$. In this case the optimal motion is:

1. Move \mathbb{A} on a shortest path from A_0 to t while avoiding $s\text{-circ}(B_0)$. If $V_0 \notin s\text{-circ}(B_1)$, this is simply a straight line and we define $[\beta_0, \beta_1] = \emptyset$. Otherwise, this involves moving \mathbb{A} to V_0 , and rotating \mathbb{A} in a range of angles $[\gamma_0, \gamma_1]$ from V_0 to t .
2. Move \mathbb{B} from B_0 to B_1 avoiding $s\text{-circ}(t)$. This involves moving \mathbb{B} to T_0 , rotating \mathbb{B} counter-clockwise about A_{int} to T_1 in a range of angles $[\alpha_0, \alpha_1]$, and then moving \mathbb{B} from T_1 to B_1 .
3. Move \mathbb{A} on a shortest path from t to A_1 while avoiding $s\text{-circ}(B_1)$. This involves rotating \mathbb{A} in a range of angles $[\gamma_2, \gamma_3]$ around $s\text{-circ}(B_1)$.

Proof. The optimality of this motion is given by Lemma 4.4, with t as the dominating point with respect to $s\text{-corr}(B_0, B_1)$. Excluding the clockwise optimal region described above is essential here, as it forces A_1 to be outside of the wedge formed by the upper tangents from A_0 to $s\text{-circ}(B_0)$ and $s\text{-circ}(B_1)$ when A_0 is below both of the B circles. This ensures that the path taken by \mathbb{A} is convex. \square

5.3 Case 3

As Case 3 is highly constrained, most of the motions for this case are particularly simple. Figures 15, 16, and 17 exhibit possible configurations of Case 3. As before, we begin by defining the zones non-constructively, and then move on to more constructive descriptions.

Let p_0 and p_1 be the upper tangent points from A_0 to $s\text{-circ}(B_0)$ and $s\text{-circ}(B_1)$ respectively. The zones are defined by the following properties:

Zone I: The set of points $q \in s\text{-corr}(B_0, B_1)$ that dominate A_0 .

Zone II: The set of points $q \in s\text{-corr}(B_0, B_1)$ A_0 dominates.

Zone III: The set of points $q \in s\text{-corr}(B_0, B_1)$ where the tangent from q to $s\text{-circ}(B_0)$ intersects $\overline{A_0 p_1}$

Zone IV: The set of points $q \in s\text{-corr}(B_0, B_1)$ where the tangent from q to $s\text{-circ}(B_1)$ intersects $\overline{A_0 p_0}$.

We do not handle situations which reduce to Case 2. For example, if $A_1 \in s\text{-corr}(B_0, B_1)$, is left of the tangent through $\overline{A_0 p_1}$, and is above $s\text{-circ}(B_0)$, then we would be in Case 2. Similarly, if $A_1 \in s\text{-corr}(B_0, B_1)$, is right of $\overline{A_0 p_1}$, and above $s\text{-circ}(B_1)$, then we would also be in Case 2.

Although Zone IV above is handled in Case 2, we keep it for symmetry. Zones I-IV of Figures 15 and 16 are defined by the following curves:

1. The two upper tangents from A_0 to $\text{circ}_s(B_0)$ and $\text{circ}_s(B_1)$ (through tangent points p_i). These tangents separate zone I from the rest of the zones. The tangent from A_0 to p_1 forms the left boundary of zone II if A_0 is below the tangent from the bottom of $\text{circ}_s(B_0)$ to the top of $\text{circ}_s(B_1)$. The tangent from A_0 to p_0 forms part of the right boundary of zone II.
2. The two horizontal tangents from $\text{circ}_s(B_0)$.
3. The lower tangent from A_0 to $\text{circ}_s(B_0)$ and $\text{circ}_s(B_1)$ (through tangent points q_i). The tangent from A_0 to q_1 (resp. q_0) form part of the right (resp. left) boundary for zone III (resp. zone IV). The tangent from A_0 to q_0 (resp. q_1) forms the left (resp. right) boundary of zone II if A_0 is above the tangent from below $\text{circ}_s(B_0)$ to above $\text{circ}_s(B_1)$ (resp. above $\text{circ}_s(B_0)$ to below $\text{circ}_s(B_1)$).
4. The arc of $\text{circ}_s(B_0)$ (resp. $\text{circ}_s(B_1)$) from p_0 to t_0 (resp. p_1 to t_1). If the tangent from A_0 to p_0 (resp. to p_1) does not intersect $\text{circ}_s(B_1)$ (resp. $\text{circ}_s(B_0)$), then t_0 is q_0 (resp. t_1 is q_1). Otherwise, t_0 (resp. t_1) is the intersection point.
5. The arc of $\text{circ}_s(B_0)$ (resp. $\text{circ}_s(B_1)$) from t_0 to q_0 (resp. t_1 to q_1). These arcs forms part of the left and right boundaries of zone II.

We now specify, for each zone, the location of A_{int} , and define T_0 and T_1 to be the lower tangent points of B_0 and B_1 to $\text{circ}_s(A_{\text{int}})$ respectively.

Zone I: A_{int} is the point A_1 .

Zone II: A_{int} is the point A_0 .

Zone III: A_{int} is the intersection point of the tangent from A_1 to the $\text{circ}_s(B_0)$ and the tangent from A_0 to $\text{circ}_s(B_1)$.

Zone IV: A_{int} is the intersection point of the tangent from A_0 to the $\text{circ}_s(B_0)$ and the tangent from A_1 to $\text{circ}_s(B_1)$.

Our generic three-stage motion then becomes:

1. Move \mathbb{A} on a straight line from A_0 to A_{int}
2. Move \mathbb{B} from B_0 to B_1 avoiding $\text{circ}_s(A_{\text{int}})$. This involves moving \mathbb{B} to T_0 , rotating \mathbb{B} counter-clockwise about A_0 to T_1 in a range of angles $[\beta_0, \beta_1]$, and then moving \mathbb{B} from T_1 to B_1 .
3. Move \mathbb{A} on a straight line motion from A_{int} to A_1 .

Note that in zone IV of Figure 15, all optimal counter-clockwise motions are of exactly the same from as zone III of Case 2.

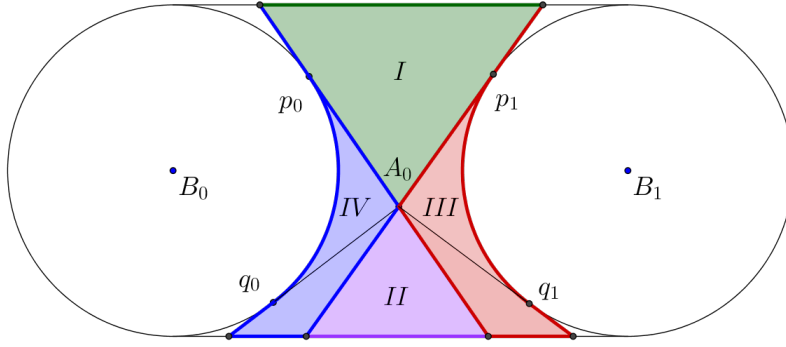


Figure 15: Case 3, when $s\text{-circ}(B_0)$ and $s\text{-circ}(B_1)$ do not intersect.

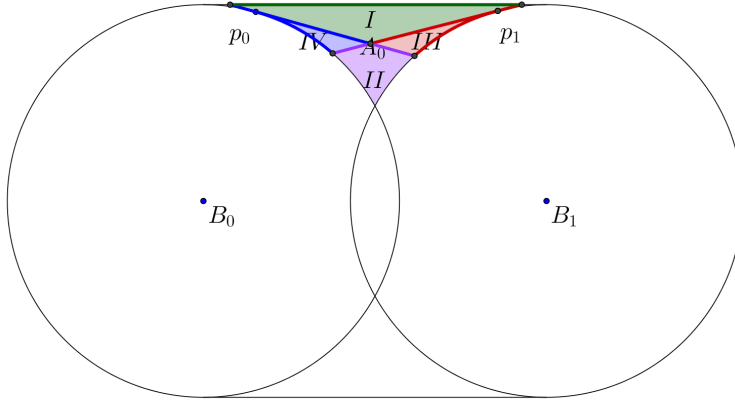


Figure 16: Case 3, when $s\text{-circ}(B_0)$ and $s\text{-circ}(B_1)$ intersect and both A_0 and A_1 are above the $s\text{-circ}(B_i)$'s.

Case 3, subcase 1: $s\text{-circ}(B_0)$ and $s\text{-circ}(B_1)$ do not intersect.

Proof. In all cases (see Figure 15), applications of Lemma 4.4 will suffice. The proof of Zones III and IV are exactly the same as the proof for Case 2, Zone III. For Zones I and II, note that for all cases that Case 2 do not cover, A_0 must be reachable from A_1 by a straight-line. Hence there are no special cases and a single application of Lemma 4.4 with either A_0 as the pivot (for Zone II) or A_1 as the pivot (for Zone I) suffices. \square

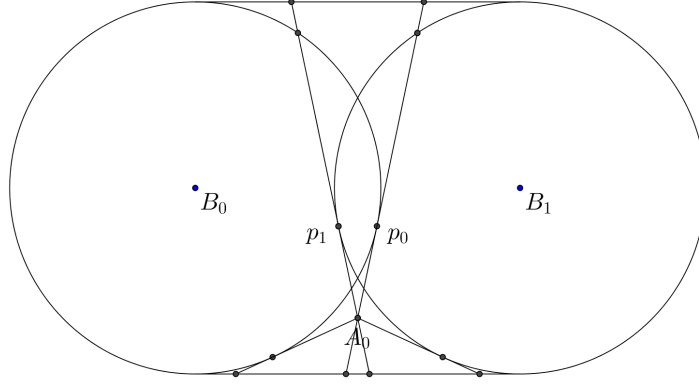


Figure 17: Case 3, when $s\text{-circ}(B_0)$ and $s\text{-circ}(B_1)$ intersect and both A_0 and A_1 are below the $s\text{-circ}(B_i)$'s.

5.3.1 Subcase 2: $s\text{-circ}(B_0)$ and $s\text{-circ}(B_1)$ intersect

When $s\text{-circ}(B_0)$ and $s\text{-circ}(B_1)$ intersect, observe that the constraints force either A_0 and A_1 to be both above the B circles, or both below. This is because if A_0 was below the $s\text{-circ}(B_i)$'s and A_1 above, then we must be in Case 2 (after possibly swapping the initial and final positions).

A_0 and A_1 both above When A_0 and A_1 are both above the B circles, we get Figure 16. In this case, the same zones and proofs as the non-intersecting case apply.

A_0 and A_1 both below When A_0 and A_1 are both below the B circles, we get Figure 17. In this case, Lemma 4.6 shows that the motion must be net-clockwise. The clockwise zones have A_0 and A_1 in the “both above” case, which is handled above.

6 Angle monotone motions

Up until now, we’ve stated all of our motions as **decoupled** motions where only one of \mathbb{A} or \mathbb{B} is moving at a time. However, we can produce angle monotone motions by simply **coupling** the optimal motions m given in the previous sections.

To be precise, let m be a motion such that $m(t_i)$ and $m(t_j)$ has the same angle. Then by coupling the motion m , we mean that we replace the submotion $m([t_i, t_j])$ with a straight-line path between $m(t_i)$ and $m(t_j)$. This process produces coupled angle monotone motions from decoupled ones. Most of the motions described in the previous section are angle monotone. The only situation in which non-angle monotonicity occurs in our decoupled motions is when A_1 is in Zone III of Case 3 above (see Figure 18). In all other cases, we have angle monotonicity for the decoupled motion as well, although the discs are possibly not be in contact for a single connected interval of time.

One can also couple the motions to achieve both angle monotonicity and the property that the two discs are in contact for a single connected interval. This is obtained by following the trace of optimal motions outlined in the previous sections while keeping \mathbb{A} and \mathbb{B} as close together as possible. The proof, although not difficult, is lengthy as it requires examining the motions of each case in the previous Section.

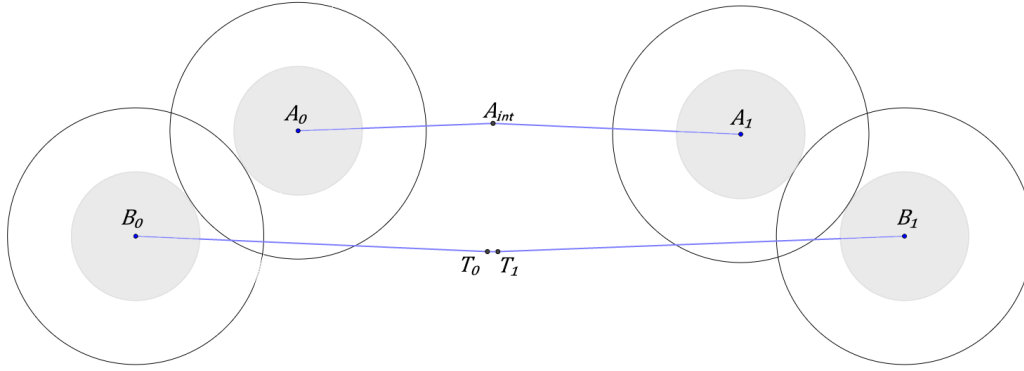


Figure 18

7 Conclusions

Using the Cauchy surface area formula, we have presented and proved shortest collision-avoiding paths for two disc robots in a planar obstacle free environment. The path lengths are neatly characterized by a simple integral, and had the property that they could be **decoupled** so that only one disc is moving at any given time, or **coupled** so that the angle formed by a ray joining the two discs changes monotonically throughout the motion. The coupled motion has the additional property that discs are in contact for a connected interval of time, that is, once the discs move out of contact, they are never in contact again.

As far as we know, our tools are limited to the case when the robots are discs in 2D. Indeed, when the robots are spheres in 3D, even if the initial and final positions of the robot reside in a common plane, we have not been able to show that the shortest path stays within this plane (except in special cases). The 3D extension of the problem as well as the 2D problem with obstacles remain subjects for future exploration.

References

- [1] Manuel Abellanas, Sergey Bereg, Ferran Hurtado, Alfredo García Olaverri, David Rappaport, and Javier Tejel. Moving coins. *Computational Geometry*, 34(1):35 – 48, 2006. Special Issue on the Japan Conference on Discrete and Computational Geometry 2004/Japan Conference on Discrete and Computational Geometry 2004.
- [2] Aviv Adler, Mark de Berg, Dan Halperin, and Kiril Solovey. *Efficient Multi-robot Motion Planning for Unlabeled Discs in Simple Polygons*, pages 1–17. Springer International Publishing, Cham, 2015.
- [3] Sergey Bereg, Adrian Dumitrescu, and János Pach. *Sliding Disks in the Plane*, pages 37–47. Springer Berlin Heidelberg, Berlin, Heidelberg, 2005.
- [4] Yui-Bin Chen and Doug Ierardi. Optimal motion planning for a rod in the plane subject to velocity constraints. In *Proceedings of the Ninth Annual Symposium on Computational Geometry*, SCG '93, pages 143–152, New York, NY, USA, 1993. ACM.
- [5] Zhengyuan Chen, Ichiro Suzuki, and Masafumi Yamashita. Time-optimal motion of two omnidirectional robots carrying a ladder under a velocity constraint. *IEEE T. Robotics and Automation*, 13(5):721–729, 1997.

- [6] Adrian Dumitrescu and Minghui Jiang. *On Reconfiguration of Disks in the Plane and Related Problems*, pages 254–265. Springer Berlin Heidelberg, Berlin, Heidelberg, 2009.
- [7] H. G. Eggleston. *Convexity*. Cambridge Tracts in Mathematics and Mathematical Physics, No. 47. Cambridge University Press, New York, 1958.
- [8] Misha Gromov. *Metric structures for Riemannian and non-Riemannian spaces*. Modern Birkhäuser Classics. English edition, 2007.
- [9] A. B. Gurevich. The "most economical" displacement of a segment (in russian). *Differentsial'nye Uravneniya*, 11(12):2134–2143, 1975.
- [10] Robert A. Hearn and Erik D. Demaine. Pspace-completeness of sliding-block puzzles and other problems through the nondeterministic constraint logic model of computation. *Theoretical Computer Science*, 343(1):72 – 96, 2005.
- [11] J E Hopcroft and G T Wolfong. Reducing multiple object motion planning to graph searching. *SIAM J. Comput.*, 15(3):768–785, August 1986.
- [12] J.E. Hopcroft, J.T. Schwartz, and M. Sharir. On the complexity of motion planning for multiple independent objects; pspace- hardness of the "warehouseman's problem". *The International Journal of Robotics Research*, 3(4):76–88, 1984.
- [13] Christian Icking, Günter Rote, Emo Welzl, and Chee-Keng Yap. Shortest paths for line segments. *Algorithmica*, 10(2-4):182–200, 1993.
- [14] Steven M. LaValle. *Planning algorithms*. Cambridge University Press, Cambridge, 2006.
- [15] Gildardo Sánchez-Ante and Jean-Claude Latombe. Using a PRM planner to compare centralized and decoupled planning for multi-robot systems. In *Proceedings of the 2002 IEEE International Conference on Robotics and Automation, ICRA 2002, May 11-15, 2002, Washington, DC, USA*, pages 2112–2119, 2002.
- [16] Jacob T Schwartz and Micha Sharir. On the piano movers' problem: III. coordinating the motion of several independent bodies: the special case of circular bodies moving amidst polygonal barriers. *The International Journal of Robotics Research*, 2(3):46–75, 1983.
- [17] Micha Sharir and Shmuel Sifrony. Coordinated motion planning for two independent robots. *Ann. Math. Artif. Intell.*, 3(1):107–130, 1991.
- [18] Kiril Solovey and Dan Halperin. On the hardness of unlabeled multi-robot motion planning. In *Robotics: Science and Systems XI, Sapienza University of Rome, Rome, Italy, July 13-17, 2015*, 2015.
- [19] Kiril Solovey, Jingjin Yu, Or Zamir, and Dan Halperin. Motion planning for unlabeled discs with optimality guarantees. *CoRR*, abs/1504.05218, 2015.
- [20] Paul G. Spirakis and Chee-Keng Yap. Strong NP-hardness of moving many discs. *Inf. Process. Lett.*, 19(1):55–59, 1984.
- [21] Trevor Standley. Finding optimal solutions to cooperative pathfinding problems. In *Proceedings of the Twenty-Fourth AAAI Conference on Artificial Intelligence, AAAI'10*, pages 173–178. AAAI Press, 2010.
- [22] Matthew Turpin, Nathan Michael, and Vijay Kumar. *Trajectory Planning and Assignment in Multirobot Systems*, pages 175–190. Springer Berlin Heidelberg, Berlin, Heidelberg, 2013.
- [23] Stanislaw Marcin Ulam. *A Collection of Mathematical Problems: Problems in Modern Mathematics*. Science Eds., 1964.

- [24] Erik I Verriest. On Ulam's problem of path planning, and "How to move heavy furniture". *IFAC Proceedings Volumes*, 44(1):14562–14566, 2011.
- [25] Glenn Wagner and Howie Choset. M*: A complete multirobot path planning algorithm with performance bounds. In *2011 IEEE/RSJ International Conference on Intelligent Robots and Systems, IROS 2011, San Francisco, CA, USA, September 25-30, 2011*, pages 3260–3267, 2011.
- [26] Chee Yap. *Coordinating the motion of several discs*. Robotics Report. Department of Computer Science, New York University, 1984.